# ProS/Mer alleviates sepsis-induced neuromuscular dysfunction by inhibiting TLR4/MyD88/NF-κB signals

**Fei Xie** ( xiefei_8896@126.com )
Sichuan Cancer Hospital & Institute, University of Electronic Science and Technology of China
**Jiaxin Sun**
Sichuan Cancer Hospital & Institute, University of Electronic Science and Technology of China
**Hongwei Zhang**
Sichuan Cancer Hospital & Institute, University of Electronic Science and Technology of China
**Shukui Zhou**
Sichuan Cancer Hospital & Institute, University of Electronic Science and Technology of China

**Research Article**

**Keywords:** microglia, Pros/Mer, toll-like receptors, sepsis, neuroinflammation

**Posted Date:** December 5th, 2022

**DOI:** https://doi.org/10.21203/rs.3.rs-2319033/v1

## Abstract

# Background

Sepsis remains a significant cause of morbidity and mortality worldwide, with systemic inflammation and behavioral impairment. Microglia are well-known critical regulators of neuroinflammation, which feature in multiple neurodegenerative disorders. These cells become “activated” through stimulation of toll-like receptors (TLRs), resulting in changes in morphology and production and release of cytokines. Myeloid-epithelial-reproductive tyrosine kinase (Mer), a member of the Tyro-Axl-Mer (TAM) family of receptor tyrosine kinases, regulates multiple features of microglial/macrophage physiology. The present study examined the roles of the related TAM receptors, Mer, and its ligand, Protein S (ProS), in regulating neuroinflammation and neuromuscular function following sepsis.

# Methods

The sepsis was established by cecal ligation and puncture (CLP) in wildtype (WT) and $Mer^{-/-}$ rats, and recombinant protein S (ProS) or normal saline (NS) was intrathecally injected for intervention. The muscle weight, neuromuscular function, Nissl staining, immunofluorescence, ELISA, and Western blot were performed.

# Results

Knockout of Mer showed significantly decreased muscle weight and neuromuscular function at day 4 post-CLP, as well as increased inflammatory cytokines, activated microglia/macrophage, and TLR4/MyD88/NF-κB signal pathway in the spinal cord. The administration of ProS activated the signal transducer and activator of transcription 1 (STAT1)/suppressor of cytokine signaling 1/3 (SOCS1/3) pathway and inhibited the TLR4/MyD88/NF-κB signal pathway, which alleviated the neuromuscular dysfunction after CLP.

# Conclusion

ProS/Mer alleviates muscle atrophy and neuromuscular dysfunction in the sepsis model by activating the STAT1/SOCS signaling pathway and inhibiting the TLR4/MyD88/NF-κB signaling pathway.

## Background

Sepsis is an infection-induced syndrome that causes devastating failure in multiple vital organs and skeletal muscle dysfunctions [1, 2]. Sepsis affects not only the peripheral muscles but also affects the central nervous system (CNS). Mechanistically, sepsis increased the permeation of the blood-spinal cord

barrier (BSCB) and blood-brain barrier (BBB) to the cytokines and bacteria; likewise, the endotheliocytes and glia were activated after the strike of ischemia of microcirculation, anoxia, and cytokines. Some studies showed that sciatic nerve inflammation progressed after spinal cord inflammation, indicating that peripheral nerve inflammation may result from spinal inflammation [3, 4].

Microglia have a vital role in regulating neuroinflammation in sepsis [5]. Microglia and perivascular macrophages activated by bacterial products are critically involved in protecting the CNS from infection [6]. The innate immune cells recognize different pathogens through the pathogen-recognition receptors (PRRs). Toll-like receptors (TLRs) are a family of PRRs that recognize conserved microbial motifs in molecules such as bacterial lipopolysaccharide (LPS) and peptidoglycan. Macrophages and microglia express TLRs that are part of the innate immune system and recognize a variety of pathogens and pathogen products[7]. TLRs, mainly TLR4, have an essential effect on modulating inflammatory responses Myeloid differentiation factor 88 (MyD88), a critical adapter protein for TLR4, which leads to the activation of downstream nuclear factor-kappa B (NF-κB) and the subsequent production of pro-inflammatory cytokines, has been implicated in neurotoxicity[8].

Moreover, after being activated, the M1-like phenotype microglia release pro-inflammatory cytokines, including tumor necrosis factors-α (TNF-α) and interleukin-6 (IL-6). On the contrary, the M2-like phenotype microglia produces anti-inflammatory factors such as interleukin-10 and transforming growth factor-β (TGF- β)[9]. Thus, a balance of pro-inflammation and anti-inflammation is responsible for the foundation of homeostasis in the CNS. Previous studies showed that the myeloid-epithelial-reproductive tyrosine kinase (Mer) regulates inflammatory responses[10, 11]. Specifically, activated Mer signaling protects the inflammatory response by switching macrophage polarization towards an M2-like phenotype[12]. It is shown that the Mer ligands, Gas6 and ProS, inhibited the TLRs-mediated inflammatory pathway in mouse-cultured microglia[13, 14]. Previous studies focused on the effect of the ProS/Mer on the TLRs signaling pathway of peripheral macrophages and dendritic cells. However, the function of Mer in regulating the inflammatory response of spinal microglia in sepsis-induced neuromuscular dysfunction has not been studied. Thus, in this study, we hypothesized that the ProS/Mer inhibits sepsis-induced spinal inflammation to alleviate peripheral neuromuscular dysfunction by inhibiting the TLR4/MyD88/NF-κB signaling pathway.

# Materials And Methods

## Animals

Adult male wild type (WT) and $Mer^{-/-}$ Sprague-Dawley (SD) rats (age: 2 months, weight range: 230–250 g) were purchased from Cyagen Co., Ltd (Guangzhou, China). According to the Animal Ethics and Use Committee of Sichuan Cancer Hospital, all rats received humane care. The rats were housed in a specific pathogen-free room under standardized conditions (25 ± 2°C, 60% humidity, and a 12 h light/dark cycle) for 1 week before the experiment. All rats had free access to food and water. All animal procedures were

performed according to the Institute Animal Care and Use Committees of the Sichuan Cancer Hospital and followed the National Institutes of Health's Guide for the Care and the Use of Laboratory Animals and the ARRIVE (Animal Research: Reporting In Vivo Experiments) guidelines, as well as recommendations of reduction, refinement, and replacement (known as the 3 Rs).

## Group Assignments And Establishment Of Sepsis Model In Rats By Clp

The WT and $Mer^{-/-}$ rats were divided into two groups: (1) the sepsis group and (2) the sham group. Each group was then divided into 2 subgroups: intrathecal injection of ProS or normal saline (NS). The sepsis model was established by cecal ligation and puncture (CLP). The sample size was calculated by our preliminary experiment and previous studies [15, 16]. We assigned 10 rats to each subgroup (Fig. 1).

The model of sepsis was induced by CLP, as previously described [17]. After anesthetized with an intraperitoneal (i.p.) injection of 0.5% sodium pentobarbital (65 mg/kg), the rats were used tail clamping to determine a sufficient depth of anesthesia. After adequate anesthesia was established, we shaved and cleaned the abdomens of the rats before performing a 2-cm-long incision through the skin and rectus abdominis on the left side of the midline to expose the cecum. We located and carefully exteriorized each rat's cecum and then ligated it with a 3–0 silk suture halfway from the base of the ileocecal valves. The ligated cecum was punctured twice with a 24-gauge needle to ensure that the wounds were infected with a small amount of stool. At last, the cecum was carefully returned to the abdomen and closed with a 3–0 silk suture. The cecum was returned to the abdomen after gentle manipulation in the sham group. In all groups, 10 mL/kg of 0.9% normal saline was subcutaneously injected after the abdomen was closed to restore the animals' fluid levels.

## Intrathecal Catheter Implantation

In this study, according to our preliminary experiments and previous studies[18], the rats were treated with an intrathecal injection of recombinant ProS (0.2 mg/kg) (9489-PS, R&D Systems) or an equal volume of NS at the 8 h, 1 day, 2 days and 3 days after CLP.

The catheter implantation was performed as described with slight modifications[19]. In brief, each rat was anesthetized with an intraperitoneal injection of 0.5% sodium pentobarbital (65 mg/kg) and placed in a prone position. A midline skin incision was made in the lumbar region (L2–S1), and the intervertebral membrane between L3 and L4 was exposed. A needle was then used to puncture the arachnoid membrane, and the PE-10 catheter was gently pushed into the subarachnoid space. The incisions were then closed in layers using 4 − 0 silk. During the surgery, the animal's core body temperature was maintained at 37 ± 0.5°C with a thermostatically controlled heating pad during surgery.

## Evaluation Of Neuromuscular Function

On day 4 after CLP, all the rats were placed in the dorsal recumbent position after anesthetization with 0.5% sodium pentobarbital (65 mg/kg). The right sciatic nerve was exposed at the thigh with non-compliant silk. Stimulation electrodes (RM6240 Systems, Inc., Chengdu, China) were attached to measure the nerve-mediated contraction of the tibialis anterior muscle with the following parameters: intensity, 3 V; duration, 0.2 ms; and frequency, 1 Hz. Compound muscle action potential (CMAP) was recorded with a receiving electrode attached to the tibialis anterior muscle before and at different times after surgery. The electromyographical data (amplitude, duration, and latency period of CMAP) were analyzed with RM6240 USB2.0S (I) version 1.0.2 software (RM6240 Systems, Chengdu Instrument Company, Chengdu, China). The motor conduction velocity (MCV) was calculated as the distance of conduction/latency time. The temperature of each rat was kept at 36–37°C using a heating light. Neuromuscular dysfunction was defined as a decrease of ≥ 20% of the lower limit of the average CMAP amplitude [20].

## Tissue Preparation

Tissue preparation was performed in our previous studies[21]. After completing the evaluation of neuromuscular function, the animals were euthanized, and muscle tissues (gastrocnemius and tibialis anterior), spinal cord (L3-4 segments), and sciatic nerve were harvested in ice-cold phosphate-buffered saline ([PBS], pH 7.40) and transferred to 4% paraformaldehyde. After a 2-day fixation, the specimens were then embedded in paraffin. The samples were cut into 4-mm-thick sections on a rotary microtome (RM2135, Leica Instruments, Wetzlar, Germany) and placed onto glass slides. The sections were deparaffinized in dimethylbenzene, rehydrated successively in a gradient of ethanol, and washed with distilled water before the subsequent experiments. The fresh frozen specimens were prepared for the other analysis.

## Enzyme-linked Immunosorbent Assay (Elisa)

The mouse TNF-α and IL-6 Enzyme-Linked Immunosorbent Assay (ELISA) Kit (CUSABIO BIOTECH Co., Ltd., China) was used following the manufacturer's instructions. In brief, the supernate of tissue was added to a 96-well plate pre-coated with hamster monoclonal anti-mouse TNF-α capture antibody. After incubation at room temperature (25℃) for 2 h, samples were washed, and the detection antibody was added for an additional hour. After further washing, avidin-horseradish peroxidase was used for detection, and optical density was measured at 450 nm and 570 nm (Multiskan GO; Thermo Fisher Scientific).

## Nissl Staining

Nissl staining was performed according to the previous study [18]. The L3-4 spinal cord slides were dehydrated with different concentration of alcohol, rehydrated in distilled water, then stained in Nissl

Staining Solution (C0117, Beyotime) for 5 min at 37°C. Subsequently, we used the 95% ethyl alcohol to immerse the slices for 5 minutes, then used 100% alcohol to dehydrated, and finally used xylene to clean slides for 5 minutes. Spinal cord slices were mounted and observed under Nikon Eclipse E800 light microscope. The average quantities of Nissl bodies (neurons with a diameter ≥ 25 μm) were counted by randomly selecting five Nissl-stained sections at the same site of each animal.

## Immunofluorescence Staining

For staining, the sections were incubated in primary antibodies made in 1% bovine serum albumin (BSA) solution to appropriate dilutions at 4 ℃ overnight. Then, the sections were washed twice, and secondary antibodies in 1% BSA were added for 1 h at room temperature. Primary antibodies were anti-Iba1 (c-32725, dilution 1:500; Santa Cruz Biotechnology, USA,) and anti-TLR4 (ab22048, dilution 1:400; Abcam, USA]. Secondary antibodies were goat anti-mouse Alexa-Fluor 594 (for Iba-1) and goat anti-mouse Alexa-Fluor 488 (for TLR4), and the stain DAPI was used at 1:400 (Invitrogen Molecular Probes). Five randomly selected sections from each group were observed using an Olympus optical microscope (BX51, Olympus, Tokyo, Japan), and 5 fields from each section were imaged for TLR4 and Iba-1 co-expression. Immunostained sections were quantitatively characterized by digital image analysis using Image Pro-Plus 6.0 software (Media Cybernetics, Bethesda, MD, USA). All the results were recorded by researchers blinded to the experimental group. TLR4 and Iba-1 were quantified as the average number of positive cells per field. A negative (no antibody) control was included.

## Western-blotting Analysis

The protein from the tissue was extracted in a lysis buffer (Beyotime Institute of Biotechnology) using sonication. The lysate was separated by centrifugation at 8, 000 × g at 4°C for 8 min, and the supernatant was collected. The total protein concentration was analyzed with the BCA Protein Assay Kit (Beyotime Institute of Biotechnology). The proteins were separated by sodium dodecyl sulfate-polyacrylamide gel electrophoresis (SDS-PAGE) and then transferred to polyvinylidene fluoride (PVDF) membranes (Millipore, Billerica). The membranes were blocked with 5% non-fat milk in Tris-buffered saline (TBS) for 1 h at room temperature (26°C), followed by overnight incubation with the following primary antibodies at 4°C: anti-Mer (1:500, 365499, Santa Cruz Biotechnology, Inc), anti-TLR4 (1:500, AF7017; Affinity Biosciences), anti-phosphorylated-STAT1 (1:500, AF3293; Affinity Biosciences), anti-p65 NF-κB (1:1000, AF5006; Affinity Biosciences), anti-SOCS 1 (1: 500, AF5378; Affinity Biosciences), anti-SOCS 3 (1: 500, AF6133; Affinity Biosciences), β-actin (1:1, 000, 47778, Santa Cruz Biotechnology, Inc) and anti-GAPDH (1:1, 000, Abcam, ab8245). After washing, the membranes were incubated with a secondary antibody (goat anti-rabbit: 1:1, 000, ZB-2301, goat anti-mouse: 1: 1, 000, ZB-2305, ZSGB-BIO) for 1 h at 37°C; the bands were visualized using the enhanced chemiluminescence kit (Beyotime, Institute of Biotechnology, Jiangsu Province, China), and the band intensity was measured using Quantity One software. All results were compared to β-actin or GAPDH to normalize the protein levels.

## Statistical Analyses

All statistical analyses were performed using SPSS (version 17.0, SPSS). Values are expressed as mean ± SD. The levels of cytokine plasma and proteins (TLR4, NF-κB, SOCS1/3, and STAT1) at 4 days after CLP were analyzed using 1-way analysis of variance (ANOVA) to compare the within-group differences, and the Student–Newman–Keuls (SNK)-q test to compare the between-group differences. The differences in all data were considered statistically significant at a *P* value less than 0.05.

# Results

## Knockout Of Mer Worsened The Muscle Atrophy And Functions After Clp

Muscle atrophy was examined by assessing muscle mass in the tibialis anterior (TA) and gastrocnemius (GC) muscles at day 4 post-CLP. The muscle weight was measured relative to pre-CLP body weight (day 0). Compared with the CLP + WT group, the TA and GC muscle weight significantly decreased in CLP + $Mer^{-/-}$ group (Fig. 2A).

The CMAP recorded for WT and $Mer^{-/-}$ group at 4 days post-CLP is shown in Fig. 2B. Compared to the CLP + WT group, the amplitudes of CMAP were significantly decreased in the CLP + $Mer^{-/-}$ group (Fig. 2C). The durations of CMAP in the CLP + $Mer^{-/-}$ group was significantly shorter than that in the CLP + WT group (Fig. 2D). The nerve conduction velocity significantly decreased in the CLP + $Mer^{-/-}$ group compared to the CLP + WT group (Fig. 2E). The latency period was significantly increased in the CLP + $Mer^{-/-}$ group compared to the CLP + WT group (Fig. 2F).

## Knockout Of Mer Aggravated Neuronal Damage And Neuromuscular Junction (Nmj) Disintegration After Clp

The Nissl and Immunofluorescence staining of the spinal cord (Fig. 3A) and skeletal muscle (Fig. 3C) were used to evaluate the neuronal damage and degeneration after CLP. In the Sham + WT group, the number of Nissl-positive neurons was observed, while in the CLP + WT group, the neurons were lightly stained and less noticeable. Moreover, knockout of Mer aggravated neuronal damage post-CLP, as demonstrated by the significant decrease in the number of Nissl-positive neurons in the spinal cord in the CLP + $Mer^{-/-}$ group compared to the CLP + WT group (Fig. 3B). Besides, CLP + WT group showed a significant decrease in the integration of NMJ, and CLP + $Mer^{-/-}$ group further aggravated disintegration of NMJ (Fig. 3D). These data indicated knockout of Mer expression aggravated neuronal damage and NMJ disintegration after CLP.

We then investigated the cellular localization and expression of TLR4 and Iba-1 in microglia/macrophages in the spinal cord at 4 days post-CLP. As demonstrated, TLR4 and Iba-1 were less

expressed in the membrane of microglia/macrophages in the Sham + WT group and Sham + Mer$^{-/-}$ group; however, TLR4 and Iba-1 were substantially upregulated in the activated microglia/macrophages in the CLP + WT group and CLP + Mer$^{-/-}$ group at 4 days post-CLP (Fig. 4A and B).

## Knockout Of Mer Aggravated The Inflammation In The Spinal Cord After Clp

As determined by ELISA, the IL-6 (Fig. 5A) and TNF-α (Fig. 5B) concentrations in the septic spinal tissue were significantly increased in the CLP + WT group compared to the Sham + WT group at 4 days after CLP. However, the IL-6 and TNF-α concentrations had no significant differences between the CLP + Mer$^{-/-}$ group and the CLP + WT group at 4 days after CLP, while they were still higher than that in the Sham + WT group and Sham + Mer$^{-/-}$ group.

### Knockout of Mer increased the TLR4 signal pathway expression and reduced STAT1 activation and SOCS1/3 expression after CLP

Our previous studies showed that the TLR4/MyD88/NF-κB signal pathway levels in the spinal cord were significantly increased at 24 h post-CLP [21]. In this study, we found that the levels of TLR4 and NF-κB were significantly increased in the CLP + WT group than in the Sham + WT group at 4 days after CLP (Fig. 6A and B). Interestingly, the levels of TLR4 and NF-κB were significantly decreased in CLP + Mer$^{-/-}$ group compared to the CLP + WT group (Fig. 6A and B).

Previous studies showed that Mer inhibits TLR4-induced inflammatory responses by activating STAT1/SOCS signaling [22]. As demonstrated, the levels of phosphorylated STAT1 (p-STAT1) were significantly increased in CLP + WT group than that in the Sham + WT group on day 4 after CLP (Fig. 6C). However, the levels of p-STAT1 were significantly decreased in CLP + Mer$^{-/-}$ group compared to CLP + WT group (Fig. 6C). Moreover, the protein expression of SOCS-1 and SOCS-3 were significantly decreased in the CLP + Mer$^{-/-}$ group when compared to the CLP + WT group (Fig. 6D and E). These findings indicated that Mer signaling is required to activate STAT1 and SOCS signaling pathways in the spinal cord after CLP.

### ProS/Mer activation alleviated functional deficits after CLP by activating STAT1 and SOCS signaling pathway and inhibiting TLR4/MyD88/NF-κB signal pathway

To further investigate the role of Mer after CLP, we used recombinant ProS (a ligand and agonist of Mer) performed at 3 h, 1 day, 2 days, and 3 days after CLP, respectively. Compared to CLP + WT + NS group, ProS treatment significantly increased the TA muscle weight (Fig. 7A) and alleviated neuromuscular dysfunction (Fig. 7B-F) at 4 days post-CLP. Furthermore, ProS treatment at 4 days post-CLP significantly decreased IL-6 and TNF-α (Suppl. Figure 1A and B) compared to CLP + WT + NS group. ProS treatment alleviated the CLP-induced neuronal damage, as demonstrated by the significant increase in the number of Nissl-positive neurons (Suppl. Figure 2A and B) and the significant increase in the integration of NMJ

(Suppl. Figure 2C and D) compared to the CLP + WT + NS group. Immunofluorescence showed that ProS treatment significantly decreased the TLR4/Iba-1 intensity compared to the CLP + WT group (Suppl. Figure 3A and B). Western blot showed that ProS treatment caused a significant decrease in TLR4 (Fig. 8A) and NF-κB (Fig. 8B) expression compared to the CLP + WT + NS group. Moreover, the ProS treatment significantly increased the expression of STAT1 (Fig. 8C), SOCS-1 (Fig. 8D), and SOCS-3 (Fig. 8E) when compared to the CLP + WT + NS group.

Interestingly, the administration of ProS could also significantly attenuate muscle atrophy (Fig. 7A) and neuromuscular dysfunction (Fig. 7B-G), decrease the expression level of TLR4 and NF-κB (Fig. 8A and B), increase the expression level of STAT1 (Fig. 8C) and SOCS1/3 (Fig. 8D and E) in CLP + $Mer^{-/-}$ group at 4 days post-CLP.

Taken together, these findings suggested that Mer promoted STAT1-mediated upregulation of SOCS expression, alleviated secondary inflammation of the spinal cord and peripheral nerve injury, and improved neuromuscular functional outcomes after CLP.

# Discussion

In this study, we demonstrated that $Mer^{-/-}$ rats had more severe muscle atrophy and neuromuscular dysfunction in a sepsis model, which is associated with increased inflammatory cytokines in the spinal cord. However, ProS/Mer significantly alleviated muscle atrophy and neuromuscular dysfunction by activating STAT1/SOCS signaling pathway and down-regulating the TLR4/MyD88/NF-κB signaling pathway.

Sepsis is a systematic inflammation that damages the function of organs and skeletal muscles [23, 24]. Sepsis-induced neuromuscular dysfunction responds to critical illness polyneuropathy and myopathy and can prolong mechanical ventilation's duration, increasing hospital stay and mortality [25]. Our previous studies not only found that sepsis can induce denervation-like alterations in NMJ [15] but also that sepsis-induced activation of spinal microglia aggravated peripheral neuromuscular dysfunction [21]. The mechanism is associated with the activation of the inflammatory signal pathway in the spinal cord.

The spinal cord, as the "superior and inferior" part of motor nerve conduction, participates in and maintains the regulation of movement. Sepsis causes inflammatory damage to peripheral nerves and can lead to various systemic disorders of the spinal cord (e.g., hypotension, hypoxemia, hyper/hypoglycemia, and organ dysfunction) [26]. Compared with the BBB, the BSCB is more sensitive to the inflammatory response because spinal cord lesions produce greater microglia/macrophage activation and more extensive leukocyte recruitment and blood-CNS barrier breakdown than comparable lesions to the cortex [27, 28]. The activated spinal microglia/macrophage results in secondary inflammation and uncontrolled inflammatory cascade in sepsis.

The activation of microglia is a central part of all types of neuroinflammatory diseases. Microglia are one of the major components of the intrinsic immune system of the spinal cord [5]. While pathogens activate the TLRs signaling, negative regulators suppress the inflammatory response to avoid excessive damage to the organism from inflammation [29]. The currently identified inflammatory negative regulators include the SOCS family and zinc finger protein A20 [30, 31]. Although the role of these negative regulators in the inflammatory response has been partially investigated, their mechanisms still need to be further clarified. The ProS/Mer system negatively regulates the inflammatory response [32, 33].

Mer is a member of the TAM family. TAM receptors are widely expressed in various mammalian immune, circulatory, and nerve cells. TAM receptors can be combined with their ligands Gas6 and ProS. The activation of the Gas6/ProS-TAM system triggers multiple downstream signal transduction pathways, which play essential roles in cell proliferation, survival, differentiation, migration, and immune function [34]. In the CNS, Tyro3 and Axl are abundantly expressed in neurons [35], whereas Mer is less defined in microglia [36]. Compared to Tyro3 and Axl receptors, $Mer^{-/-}$ mice showed significantly increased lethality by lipopolysaccharide, which may be related to endotoxin-induced overexpression of TNF-α [37]. In addition, the functions of ProS and Gas6 are different; for example, ProS directly activates the Mer receptor, whereas Gas6 does not [38]. Therefore, in the Mer receptor-mediated inhibition of inflammatory responses, ProS may have a more critical role than Gas6 in the Mer receptor-mediated inhibition of inflammatory responses [39].

There are still some limitations in our study. Firstly, the phenotypes of microglia are not distinguished. Microglia can be activated from an M1-like phenotype to an M2-like phenotype after an inflammatory injury. We used Iba-1 to mark microglia/macrophages in the current study but did not classify the cells. Peripheral immune infiltration and alterations can also significantly impact sepsis [40]. However, our results showed that the administration of ProS significantly increased the percentage of Arg-1 in $Mer^{-/-}$ and WT cells after LPS treatment (Suppl. Figure 4). These findings indicated that ProS/Mer plays a vital role in regulating microglial/macrophage M1/M2 polarization, and the absence of Mer expression tips the balance of microglial/macrophage activation towards the pro-inflammatory M1-like phenotype. Secondly, we have used only $Mer^{-/-}$ rats to investigate pro-inflammatory and anti-inflammatory responses. However, we aimed to clarify the role of Mer in regulating a pro- or anti-inflammatory mechanism, and the critical mechanism of TAM receptors involved in the TLRs response needs to be completed in the future. Furthermore, the other knocked-out receptors ($Tyro3^{-/-}$ and $Axl^{-/-}$) could be used to confirm any ligand-dependent roles of the TAM receptors that occur under basal conditions in microglial cells. Interestingly, even though in the $Mer^{-/-}$ rats, ProS treatment also can alleviate neuromuscular dysfunction and upregulated the expression of STAT1 and SOCS1/3. It seems likely that ProS could activate the other two receptors to play the anti-inflammation role. Nevertheless, our data show the clear modulatory part of ProS under pro-inflammatory conditions, which is this study's main finding.

# Conclusions

In conclusion, our study demonstrated that knockout of Mer significantly increases inflammatory cytokines release, contributing to the aggravation of muscle atrophy and neuromuscular dysfunction after sepsis. The activation of Mer has beneficial effects on sepsis by upregulating STAT/SOCS signaling pathway and inhibiting the TLR4/MyD88/NF-κB signaling pathway.

# Abbreviations

ANOVA
analysis of variance
BBB
blood-brain barrier
BSCB
blood-spinal cord barrier
CLP
cecal ligation and puncture
CMAP
compound muscle action potential
CNS
central nervous system
DAPI
4',6-diamidino-2-phenylindole
ELISA
enzyme-linked immunosorbent assay
Gas6
Growth arrest-specific factor 6
LPS
lipopolysaccharide
Mer
myeloid-epithelial-reproductive tyrosine kinase
MCV
motor conduction velocity
NF-κB
nuclear factor-kappa B
NS
normal saline
PBS
phosphate-buffered saline
ProS
Protein S
PRRs

pattern recognition receptors
PVDF
polyvinylidene fluoride
SD rats
Sprague-Dawley rats
SDS-PAGE
sodium dodecyl sulfate polyacrylamidegel electrophoresis
SNK
student–newman–keuls
SOCS1/3
suppressor of cytokine signaling 1/3
STAT1
signal transducer and activator of transcription 1
TLR
Toll-like receptor
TNF-α
tumor necrosis factor alpha.

# Declarations


### Funding

This work was supported by the National Natural Science Foundation of China (No. 81901276) and the Natural and Science Foundation of Sichuan Province (2020YJ0177).


### Competing interests

The authors declare that they have no competing interests.


### Acknowledgments

Not applicable.


### Availability of data and materials

All data generated or analyzed during this study are included in this published article.

### Authors' contributions

FX contributed to the design and conduction of this study, data analysis, and writing and approved the final manuscript. JX S and HW Z participated in establishing the animal model and recording muscular function. SK Z recorded molecular biology results and analyzed the data. SK Z read the manuscript and gave suggestions. All authors read and approved the final manuscript.

### Consent for publication

Not applicable.

### Ethics approval

Human subjects or samples were not used in this study. All animal experiments were approved by the Institute Animal Care and Use Committees of the Sichuan Cancer Hospital.

# References


1. Purcarea A, Sovaila S. Sepsis. a 2020 review for the internist. Rom J Intern Med. 2020;58(3):129–37.
2. Lv B, Min S, Xie F, Yang J, Chen J. Alleviating Sepsis-Induced Neuromuscular Dysfunction Linked With Acetylcholine Receptors by Agrin. J Surg Res. 2019;241:308–16.
3. Graber DJ, Hickey WF, Harris BT. Progressive changes in microglia and macrophages in spinal cord and peripheral nerve in the transgenic rat model of amyotrophic lateral sclerosis. J Neuroinflammation. 2010;7:8.
4. Trolese MC, Scarpa C, Melfi V, et al. Boosting the peripheral immune response in the skeletal muscles improved motor function in ALS transgenic mice. Mol Ther. 2022;30(8):2760–84.
5. Aloisi F. Immune function of microglia. Glia. 2001;36(2):165–79.
6. Norden DM, Muccigrosso MM, Godbout JP. Microglial priming and enhanced reactivity to secondary insult in aging, and traumatic CNS injury, and neurodegenerative disease. Neuropharmacology. 2015;96(Pt A):29–41.
7. Zhang CJ, Jiang M, Zhou H, et al. TLR-stimulated IRAKM activates caspase-8 inflammasome in microglia and promotes neuroinflammation. J Clin Invest. 2018;128(12):5399–412.
8. Hu N, Wang C, Dai X, et al. Phillygenin inhibits LPS-induced activation and inflammation of LX2 cells by TLR4/MyD88/NF-κB signaling pathway. J Ethnopharmacol. 2020;248:112361.
9. Pisanu A, Lecca D, Mulas G, et al. Dynamic changes in pro- and anti-inflammatory cytokines in microglia after PPAR-γ agonist neuroprotective treatment in the MPTPp mouse model of progressive Parkinson's disease. Neurobiol Dis. 2014;71:280–91.
10. Cai B, Thorp EB, Doran AC, et al. MerTK cleavage limits proresolving mediator biosynthesis and exacerbates tissue inflammation. Proc Natl Acad Sci U S A. 2016;113(23):6526–31.
11. Healy LM, Perron G, Won SY, et al. MerTK Is a Functional Regulator of Myelin Phagocytosis by Human Myeloid Cells. J Immunol. 2016;196(8):3375–84.
12. Myers KV, Amend SR, Pienta KJ. Targeting Tyro3, Axl and MerTK (TAM receptors): implications for macrophages in the tumor microenvironment. Mol Cancer. 2019;18(1):94.
13. Gilchrist SE, Goudarzi S, Hafizi S. Gas6 Inhibits Toll-Like Receptor-Mediated Inflammatory Pathways in Mouse Microglia via Axl and Mer. Front Cell Neurosci. 2020;14:576650.

14. Ubil E, Caskey L, Holtzhausen A, Hunter D, Story C, Earp HS. Tumor-secreted Pros1 inhibits macrophage M1 polarization to reduce antitumor immune response. J Clin Invest. 2018;128(6):2356–69.
15. Liu L, Xie F, Wei K, et al. Sepsis induced denervation-like changes at the neuromuscular junction. J Surg Res. 2016;200(2):523–32.
16. Xie F, Min S, Liu L, Peng L, Hao X, Zhu X. Advanced age enhances the sepsis-induced up-regulation of the γ- and α7-nicotinic acetylcholine receptors in different parts of the skeletal muscles. Arch Gerontol Geriatr. 2016;65:1–8.
17. Rittirsch D, Huber-Lang MS, Flierl MA, Ward PA. Immunodesign of experimental sepsis by cecal ligation and puncture. Nat Protoc. 2009;4(1):31–6.
18. Wu H, Zheng J, Xu S, et al. Mer regulates microglial/macrophage M1/M2 polarization and alleviates neuroinflammation following traumatic brain injury. J Neuroinflammation. 2021;18(1):2.
19. Loram LC, Harrison JA, Chao L, et al. Intrathecal injection of an alpha seven nicotinic acetylcholine receptor agonist attenuates gp120-induced mechanical allodynia and spinal pro-inflammatory cytokine profiles in rats. Brain Behav Immun. 2010;24(6):959–67.
20. Van den Bergh PY, Piéret F. Electrodiagnostic criteria for acute and chronic inflammatory demyelinating polyradiculoneuropathy. Muscle Nerve. 2004;29(4):565–74.
21. Xie F, Min S, Chen J, Yang J, Wang X. Ulinastatin inhibited sepsis-induced spinal inflammation to alleviate peripheral neuromuscular dysfunction in an experimental rat model of neuromyopathy. J Neurochem. 2017;143(2):225–35.
22. Rothlin CV, Ghosh S, Zuniga EI, Oldstone MB, Lemke G. TAM receptors are pleiotropic inhibitors of the innate immune response. Cell. 2007;131(6):1124–36.
23. Hermans G, Van den Berghe G. Clinical review: intensive care unit acquired weakness. Crit Care. 2015;19(1):274.
24. Cohen S, Nathan JA, Goldberg AL. Muscle wasting in disease: molecular mechanisms and promising therapies. Nat Rev Drug Discov. 2015;14(1):58–74.
25. Farivar BS, Eiref SD, Leitman IM. Strategies to prevent sepsis-induced intensive care unit-acquired weakness: are there any options? Commentary on "Comparison of melatonin and oxytocin in the prevention of critical illness polyneuropathy in rats with surgically induced sepsis". J Surg Res. 2013;185(1):e39–42.
26. Ahmed WA, de Heredia LL, Hughes RJ, Belci M, Meagher TM. Outcomes of whole-body computed tomography in spinal cord-injured patients with sepsis. Spinal Cord. 2014;52(7):536–40.
27. Kopper TJ, Gensel JC. Myelin as an inflammatory mediator: Myelin interactions with complement, macrophages, and microglia in spinal cord injury. J Neurosci Res. 2018;96(6):969–77.
28. Azizi F, Ghasemi R, EbrahimiBarough S, Ardalan M, Hadjighassem M. Effect of multifactorial therapeutic approach on axonal regeneration and cell viability in an in-vitro model of spinal-derived neural injury. Cell Tissue Bank. 2022.

29. Liew FY, Xu D, Brint EK, O'Neill LA. Negative regulation of toll-like receptor-mediated immune responses. Nat Rev Immunol. 2005;5(6):446–58.
30. Ecco G, Imbeault M, Trono D. KRAB zinc finger proteins. Development. 2017;144(15):2719–29.
31. Yoshimura A, Ito M, Chikuma S, Akanuma T, Nakatsukasa H. Negative Regulation of Cytokine Signaling in Immunity. Cold Spring Harb Perspect Biol. 2018. 10(7).
32. Law LA, Graham DK, Di Paola J, Branchford BR. GAS6/TAM Pathway Signaling in Hemostasis and Thrombosis. Front Med (Lausanne). 2018;5:137.
33. Bellan M, Pirisi M, Sainaghi PP. The Gas6/TAM System and Multiple Sclerosis. Int J Mol Sci. 2016. 17(11).
34. Huang Y, Yoon MK, Otieno S, Lelli M, Kriwacki RW. The activity and stability of the intrinsically disordered Cip/Kip protein family are regulated by non-receptor tyrosine kinases. J Mol Biol. 2015;427(2):371–86.
35. Lai C, Lemke G. An extended family of protein-tyrosine kinase genes differentially expressed in the vertebrate nervous system. Neuron. 1991;6(5):691–704.
36. Ji R, Tian S, Lu HJ, et al. TAM receptors affect adult brain neurogenesis by negative regulation of microglial cell activation. J Immunol. 2013;191(12):6165–77.
37. Camenisch TD, Koller BH, Earp HS, Matsushima GK. A novel receptor tyrosine kinase, Mer, inhibits TNF-alpha production and lipopolysaccharide-induced endotoxic shock. J Immunol. 1999;162(6):3498–503.
38. Tibrewal N, Wu Y, D'mello V, et al. Autophosphorylation docking site Tyr-867 in Mer receptor tyrosine kinase allows for dissociation of multiple signaling pathways for phagocytosis of apoptotic cells and down-modulation of lipopolysaccharide-inducible NF-kappaB transcriptional activation. J Biol Chem. 2008;283(6):3618–27.
39. Weinger JG, Gohari P, Yan Y, Backer JM, Varnum B, Shafit-Zagardo B. In brain, Axl recruits Grb2 and the p85 regulatory subunit of PI3 kinase; in vitro mutagenesis defines the requisite binding sites for downstream Akt activation. J Neurochem. 2008;106(1):134–46.
40. Walker PA, Shah SK, Jimenez F, Aroom KR, Harting MT, Cox CS Jr. Bone marrow-derived stromal cell therapy for traumatic brain injury is neuroprotective via stimulation of non-neurologic organ systems. Surgery. 2012;152(5):790–3.

# Figures

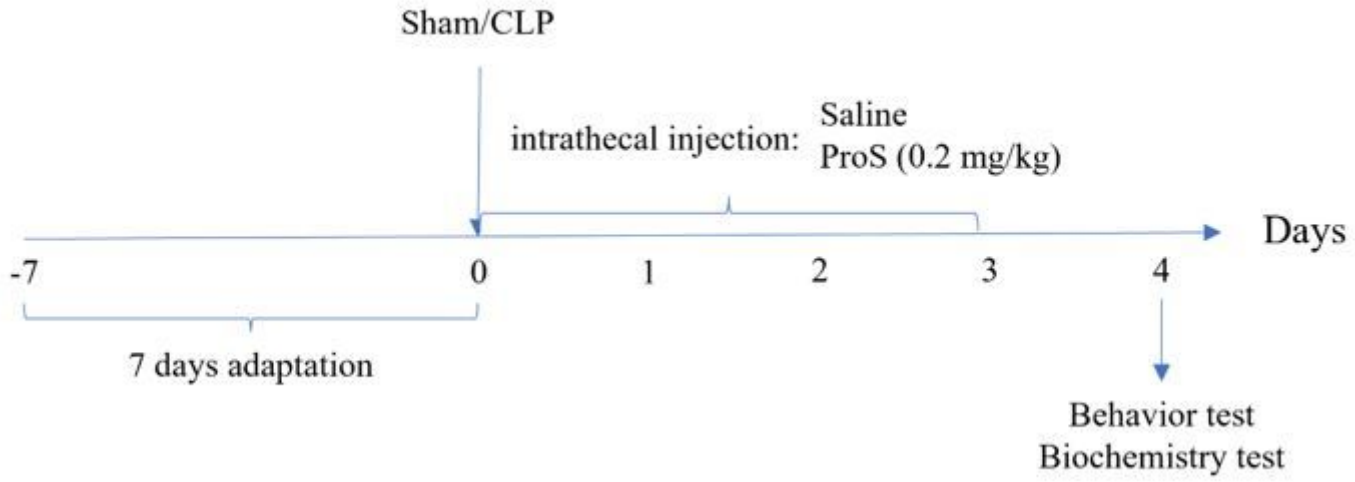


**Figure 1**

**Experimental Design.** After 7 days adaptation, on day 0, cecal ligation and puncture (CLP) or sham operation was produced. Drug treatments were started 8 h after CLP or sham and consisted of administering a single dose of saline or ProS (0.2 mg/kg). On the subsequent 3 days, saline (equal volume) or ProS (0.2 mg/kg) was administered to the CLP or sham group. Behavior tests (CMAP) and biochemistry tests were performed on day 4 on CLP and sham rats.

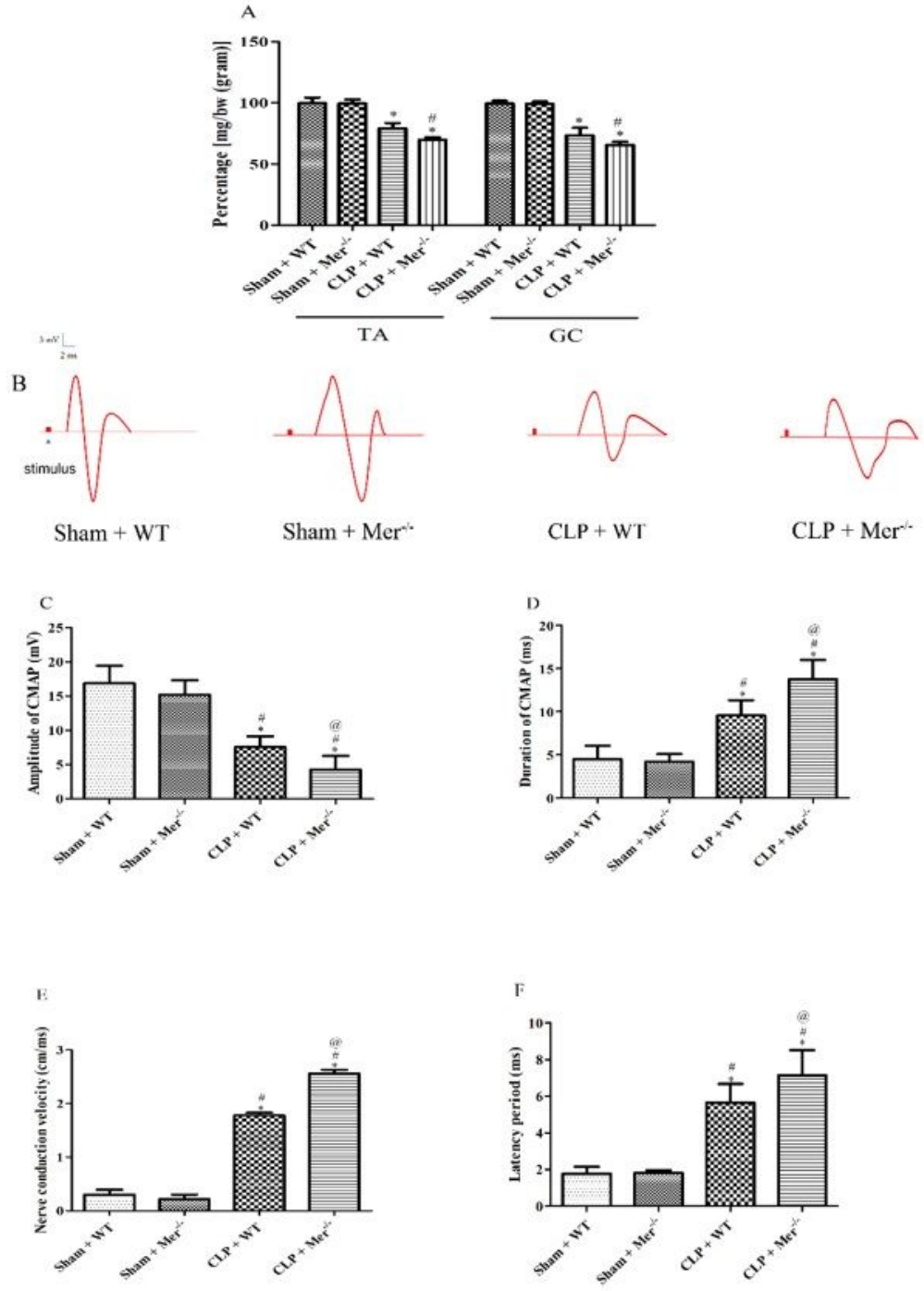


## Figure 2

**Knockdown of Mer worsened the muscular function outcomes after CLP.** (A) The changes in muscle weight of Sham + WT, Sham + Mer, CLP + WT, and CLP + Mer groups were performed on day 4 after CLP. Muscle weights are expressed as a ratio to body weight pre-CLP. CLP significantly increased muscle wasting in the WT group and aggravated the neuromuscular dysfunction in $Mer^{-/-}$ group. Data are shown as mean ± SD. n = 5 rats per group. (B) Samples of the CMAPs were recorded on day 4 after CLP in Sham

+ WT, Sham + Mer, CLP + WT, and CLP + Mer groups. Compared to the Sham + WT group, CLP significantly decreased the amplitude (C) and increased the durations, nerve conduction velocity, and latency period (D, E, and F) in the WT group. Knockout of Mer worsened the CMAP outcomes after CLP. Data are shown as mean ± SD. n = 5 rats per group. $^{*}P < 0.05$ compared to Sham + WT group, $^{\#}P < 0.05$ compared to Sham + Mer$^{-/-}$ group, $^{@}P < 0.05$ compared to CLP + WT group.

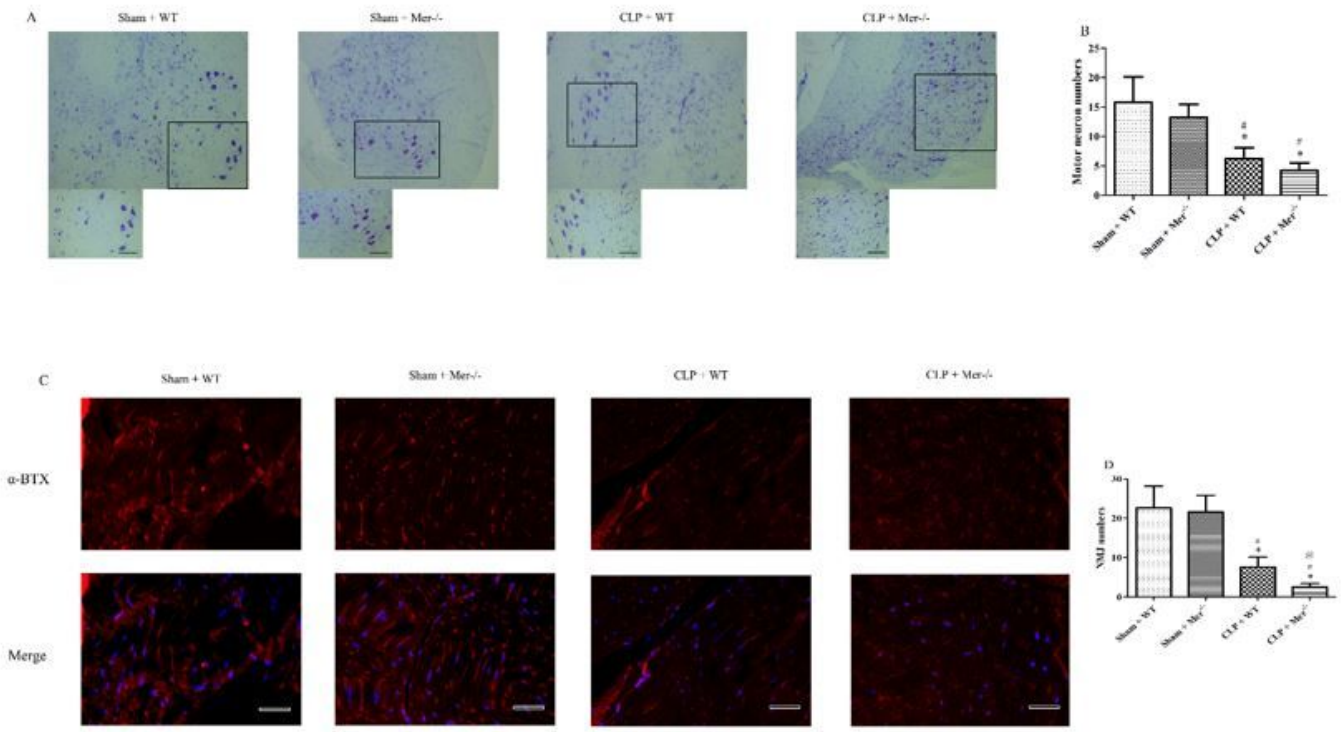


## Figure 3

**Knockout of Mer decreased the neuronal numbers and NMJ numbers after CLP.** (A) Representative images of Nissl staining in the ventral horn of the spinal cord from the Sham + WT, Sham + Mer, CLP + WT, and CLP + Mer groups, respectively. The Nissl bodies were observed with dark blue staining in the Sham + WT group. However, in the CLP + WT group, Nissl bodies were less obvious with lighter staining. Knockout of Mer decreased the Nissl bodies after CLP. n = 5 rats per group. (B) The motor neuron numbers in the ventral horn of each group were quantified. CLP significantly decreased neuron numbers and aggravated the loss of neuron numbers in the Mer$^{-/-}$ group. Data are shown as mean ± SD. n = 5 rats per group. (C) Representative images of immunofluorescence staining in the synaptic membrane from the Sham + WT, Sham + Mer, CLP + WT, and CLP + Mer groups, respectively. n = 5 rats per group. (D) Quantification analysis showed CLP significantly decreased the number of NMJ in the synaptic membrane at day 4 after CLP, and knockout of Mer further decreased the number of NMJ in the synaptic membrane after CLP. Data are shown as mean ± SD. n = 5 rats per group. $^{*}P < 0.05$ compared to Sham + WT group, $^{\#}P < 0.05$ compared to Sham + Mer$^{-/-}$ group, $^{@}P < 0.05$ compared to CLP + WT group.

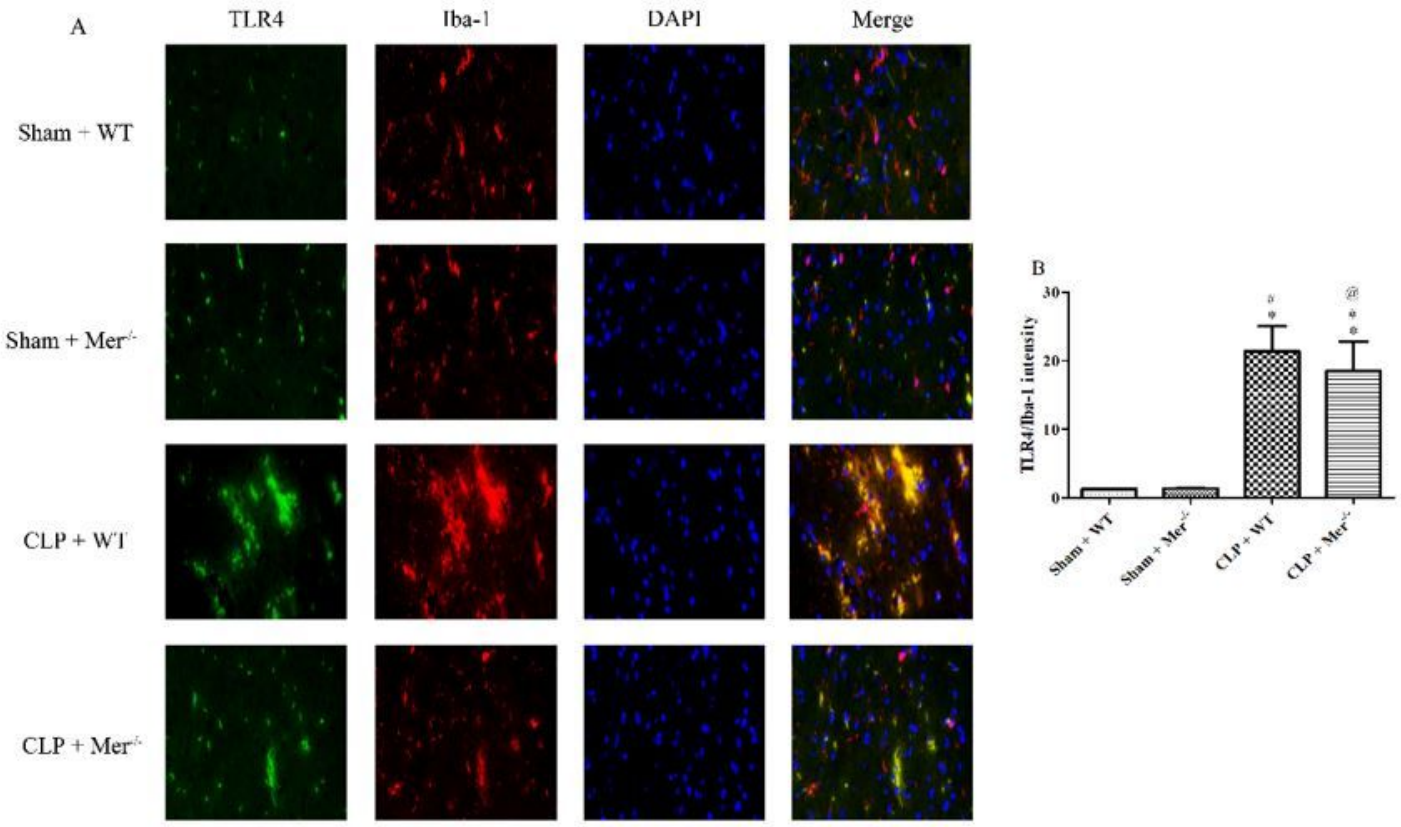


## Figure 4

**Knockout of Mer activated the Iba-positive cells co-labeled with TLR4 at day 4 after CLP.** (A) Representative Iba-1-positive cells co-labeled with TLR4 in the septic spinal tissue at day 4 after CLP. (B) Quantification showed that the Sham + WT rats had significantly fewer Iba-1-positive cells co-labeled with TLR4 in the spinal tissue than the CLP + WT rats and CLP + Mer$^{-/-}$ rats. The total number of Iba-1-positive cells co-labeled with TLR4 is expressed as the mean number per field of view. Data are shown as mean ± SD. n = 5 rats per group. Bar = 100 μm. $^{*}P < 0.05$ compared to Sham + WT group, $^{\#}P < 0.05$ compared to Sham + Mer$^{-/-}$ group, $^{@}P < 0.05$ compared to CLP + WT group.

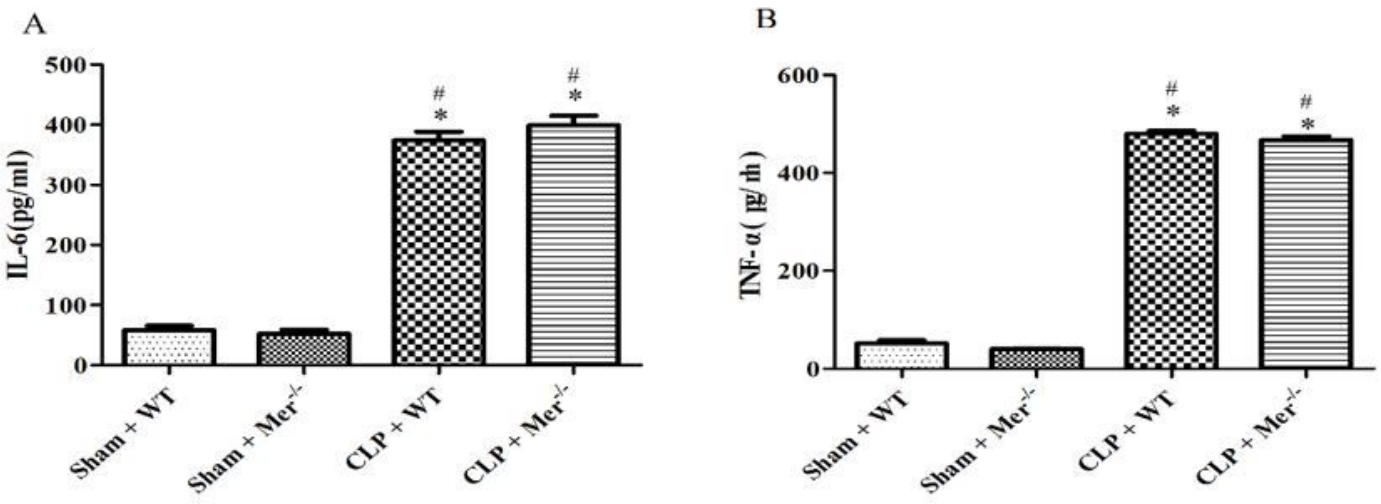


## Figure 5

**Knockout of Mer significantly increased the level of cytokines in the spinal cord after CLP.** ELISA showed that the release of IL-6 and TNF-α (C and D) in the spinal cord at day 4 after CLP was significantly increased in WT and $Mer^{-/-}$ groups. Data are shown as mean ± SD. n = 5 rats per group. $^{*}P < 0.05$ compared to Sham + WT group, $^{\#}P < 0.05$ compared to Sham + $Mer^{-/-}$ group, $^{@}P < 0.05$ compared to CLP + WT group.

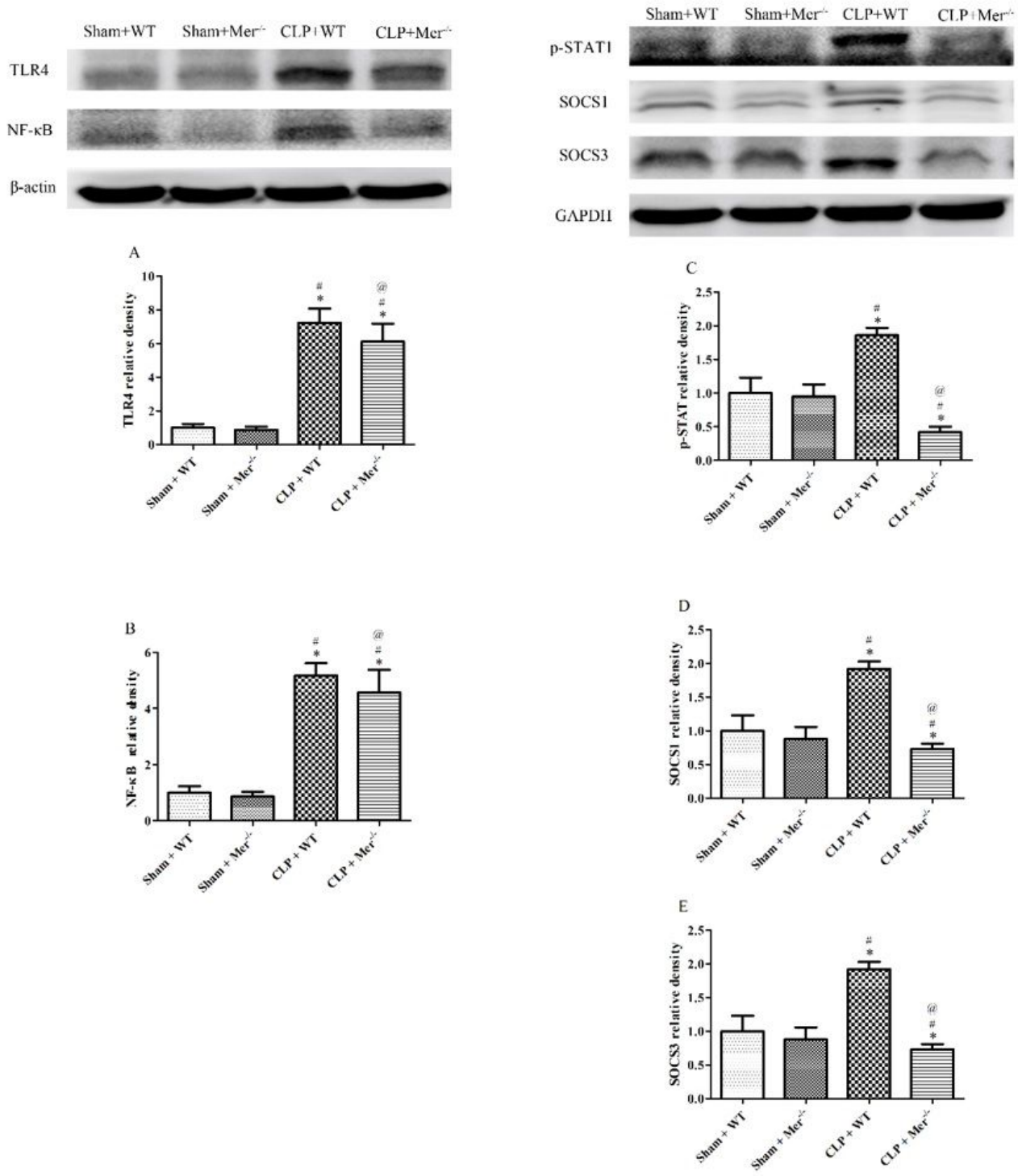


## Figure 6

**Knockout of Mer reduced STAT1 activation and SOCS expression after CLP.** Representative immunoblots and quantification showing the expression of TLR4 (A), NF-κB (B) was significantly increased in WT and $Mer^{-/-}$ group at day 4 after CLP; however, the expression of phosphorylated STAT1 (p-STAT1) (C), SOCS1 (D), and SOCS3 (E) were significantly decreased at day 4 after CLP. Data are expressed as fold change

compared to the Sham + WT group; n = 5 rats per group. $^{*}P < 0.05$ compared to Sham + WT group, $^{\#}P < 0.05$ compared to Sham + Mer$^{-/-}$ group, $^{@}P < 0.05$ compared to CLP + WT group.

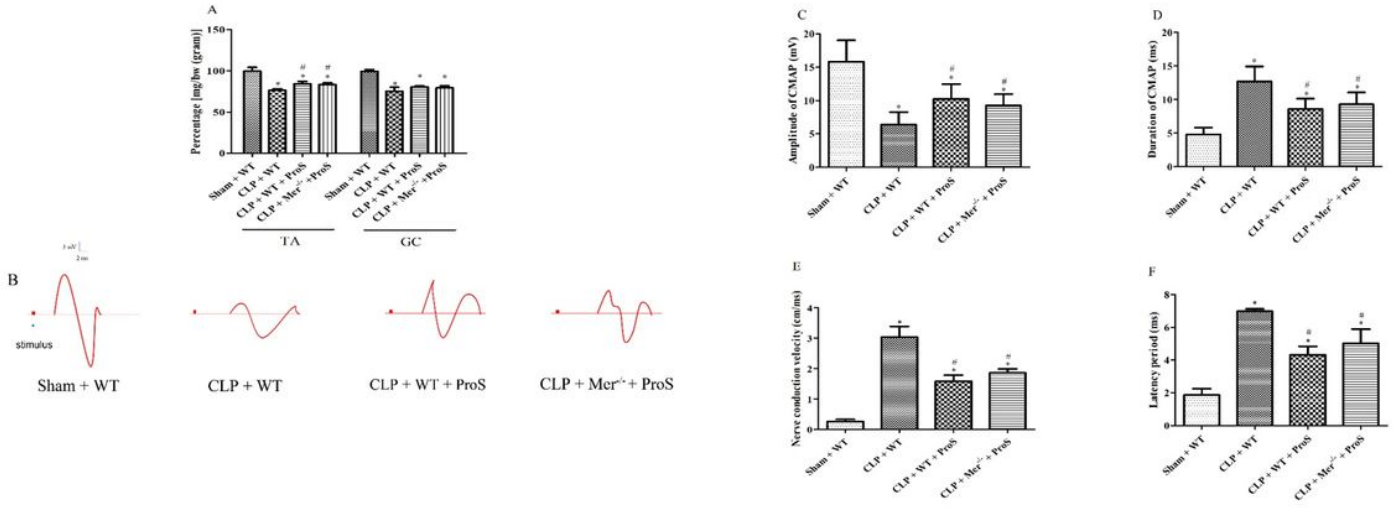


## Figure 7

**Mer activation alleviated the muscular dysfunction outcomes after CLP.** (A) The changes in muscle weight of Sham + WT, CLP + WT, CLP + WT + ProS, and CLP + Mer$^{-/-}$ + ProS groups were performed on day 4 after CLP. The administration of ProS significantly decreased muscle wasting and alleviated the neuromuscular dysfunction in Mer$^{-/-}$ group. Data are shown as mean ± SD. n = 5 rats per group. (B) Samples of the CMAPs recorded on day 4 after CLP in Sham + WT, CLP + WT, CLP + WT + ProS, and CLP + Mer$^{-/-}$ + ProS groups. Compared to the CLP + WT group, ProS significantly increased the amplitude (C) and decreased the durations, nerve conduction velocity, and latency period (D, E, and F) in the WT group but not significant in Mer$^{-/-}$ group after CLP. Data are shown as mean ± SD. n = 5 rats per group. $^{*}P < 0.05$ compared to Sham + WT group, $^{\#}P < 0.05$ compared to CLP + WT group.

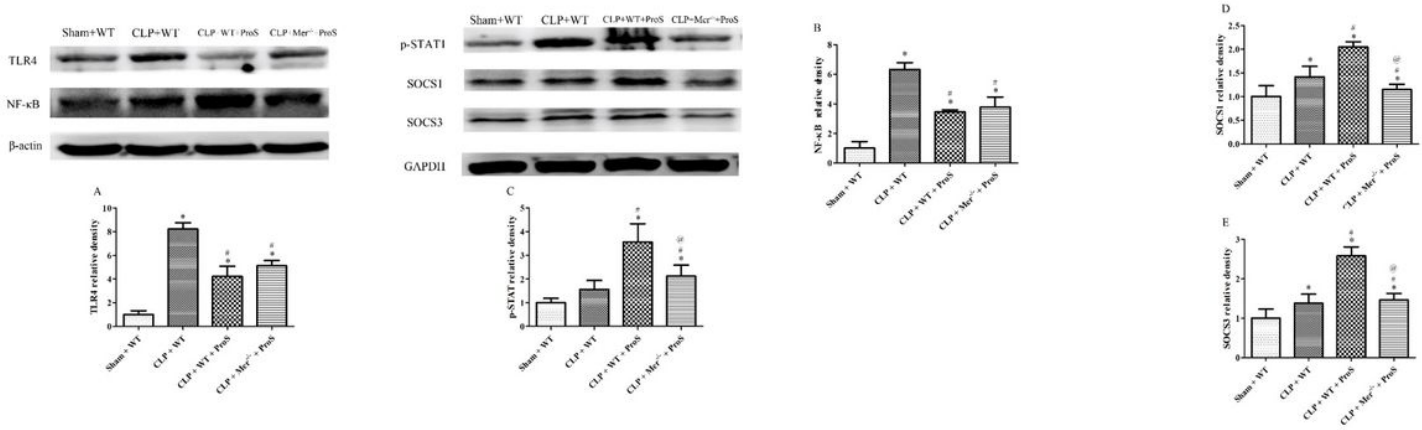


## Figure 8

**Mer activation reduced TLR4 activation and increased STAT1 and SOCS expression after CLP.** Representative immunoblots and quantification showing the administration of ProS significantly decreased the expression of TLR4 (A), NF-κB (B) and increased the expression of phosphorylated STAT1 (p-STAT1) (C), SOCS-1 (D), and SOCS-3 (E) in WT and $Mer^{-/-}$ group at day 4 after CLP. Data are expressed as fold change compared to the Sham + WT group; n = 5 rats per group. $^{*}P < 0.05$ compared to Sham + WT group, $^{\#}P < 0.05$ compared to CLP + WT group, $^{@}P < 0.05$ compared to CLP + WT + ProS group.

# Supplementary Files

This is a list of supplementary files associated with this preprint. Click to download.

- Suppl.Fig1.tif
- Suppl.Fig2.tif
- Suppl.Fig3.tif
- Suppl.Fig4.tif
- WBrecords.docx